Available online at www.sciencedirect.com
ScienceDirect
Thin Solid Films 516 (2008) 1523–1528
www.elsevier.com/locate/tsf

ZnO thin films prepared by atomic layer deposition and rf sputtering as an active layer for thin film transistor

S.J. Lim, Soonju Kwon, H. Kim *

Department of Materials Science and Engineering, POSTECH, San 31, Hyoja-Dong, Nam-Gu, Pohang, 790-784, Republic of Korea

Available online 3 April 2007

Abstract

Recently, the application of ZnO thin films as an active channel layer of transparent thin film transistor (TFT) has become of great interest. In this study, we deposited ZnO thin films by atomic layer deposition (ALD) from diethyl Zn (DEZ) as a metal precursor and water as a reactant at growth temperatures between 100 and 250 °C. At typical growth conditions, pure ZnO thin films were obtained without any detectable carbon contamination. For comparison of key film properties including microstructure and chemical and electrical properties, ZnO films were also prepared by rf sputtering at room temperature. The microstructure analyses by X-ray diffraction have shown that both of the ALD and sputtered ZnO thin films have (002) preferred orientation. At low growth temperature $T_s \leq 125$ °C, ALD ZnO films have high resistivity (>10 Ω cm) with small mobility (<3 cm^2/V s), while the ones prepared at higher temperature have lower resistivity (<0.02 Ω cm) with higher mobility (>15 cm^2/V s). Meanwhile, sputtered ZnO films have much higher resistivity than ALD ZnO at most of the growth conditions studied. Based upon the experimental results, the electrical properties of ZnO thin films depending on the growth conditions for application as an active channel layer of TFT were discussed focusing on the comparisons between ALD and sputtering.

Keywords: Atomic layer deposition; rf sputtering; ZnO; Transparent TFT

1. Introduction

ZnO is one of the typical transparent conducting oxides with a number of great characteristics; large band gap (3.36 eV), low dielectric constant, large exciton binding energy (60 meV), and good photoelectric and piezoelectric properties. Thus, ZnO has been studied for various applications including gas sensors [1], transducers [2], heaters and defrosters [3], solar cells [4], diluted magnetic semiconductors (DMS) [5] electronic and optoelectronic devices such as ultraviolet photodetector [6], light-emitting diodes (LED) [7], surface acoustic wave devices (SAW) [8], and transparent electrodes [9,10]. Recently, the application of ZnO as an active channel layer of transparent thin film transistor (TTFT) has attracted great interest since ZnO can be prepared at low deposition temperature with relatively high field effect mobility (0.2–40 cm^2/V s), good on–off ratio of about 10^3–10^6, and transparency within visible range wave length [11–18]. While a great number of various deposition techniques were reported for ZnO thin films, most of the ZnO active layers in TFT have been deposited by physical vapor deposition methods such as sputtering or pulsed laser deposition (PLD) [11–16,19].

Atomic layer deposition (ALD) is a gas-phase thin film deposition method characterized by the alternate exposure of chemical species with self-limiting surface reactions, producing films with accurate thickness control, excellent conformality, and uniformity over large areas [20]. Especially, ALD can produce high quality films at relatively low temperature, which makes it very attractive for active channel layer deposition of TFT. While ALD of Ga-, B-, and Al-doped ZnO thin films were reported previously for applications as transparent conducting oxide [21–24], the ALD of intrinsic ZnO has been relatively rarely studied [25]. In this study, we prepared ZnO films with ALD using diethyl Zn (DEZ) as a metal precursor and water as a reactant. Key film properties including microstructure and chemical and electrical properties were characterized and compared with ZnO films prepared by rf sputtering focusing on the application as an active channel layer of TFT.

* Corresponding author.
E-mail addresses: lsjwlb@postech.ac.kr (S.J. Lim), hyungjun@postech.ac.kr (H. Kim).

0040-6090/$ - see front matter © 2007 Elsevier B.V. All rights reserved.
doi:10.1016/j.tsf.2007.03.144

2. Experimental details

A homemade transverse flow type ALD reactor was used for ALD of ZnO thin films. Fig. 1 is a schematic drawing of ALD system. Substrate is heated by halogen lamp located outside of quartz tube chamber body, providing growth temperature up to 500 °C. DEZ, Epichem adduct grade, was used as a metal precursor and water vapor without bubbling was used as a reactant. Ar was used as a purging and carrier gas, whose inlet was separated at the side of the chamber. The Ar flow was controlled by mass flow controller (5.5 sccm for DEZ bubbler and 60 sccm for purging). For constant flowing of water, the temperature of water container was maintained at 65 °C. DEZ bubbler temperature was maintained at 13 °C by using a cooling circulator, producing vapor pressure of 1066 Pa. To prevent possible problems caused by the very high pressure of DEZ, the bubbler pressure was set to 5.46×10^{4} Pa by using Ar. The flows of precursor and reactant were controlled by needle valve to set the pressure of the reactor to 40 Pa for water and 17.3 Pa for DEZ flowing step. ALD ZnO films were deposited at the growth temperature range from 100 °C to 250 °C. Typical ALD ZnO growth sequence is composed of 2 s of DEZ exposure, 8 s of Ar purging, 3 s of H_2O exposure, and 4 s of Ar purging. Typically, the number of ALD cycles was 200 times.

The sputtering system is equipped with three sputter guns, two DCs and one rf, enabling co-sputtering. For this work, rf sputtering was used by using 5.06-cm-diameter ZnO target with 99.99% purity. The distance from the target to the substrate was 9.5 cm and the base pressure was 6.66×10^{-4} Pa. Deposition was conducted at room temperature with varying sputtering power (50, 100, and 150 W) and working pressure (0.2, 0.67, and 1.33 Pa). The substrate was rotated with 20–25 rpm during film deposition and pre-sputtering was conducted before deposition to remove contamination on target surface.

The substrates were corning glass 1737 and Si(001) substrate. While the glass substrates were cleaned by consequential dipping in trichloroethylene, acetone, and methanol, respectively, for 10 min, the Si substrates were cleaned by degreasing using acetone, IPA, and water followed by dipping in 1% HF solution

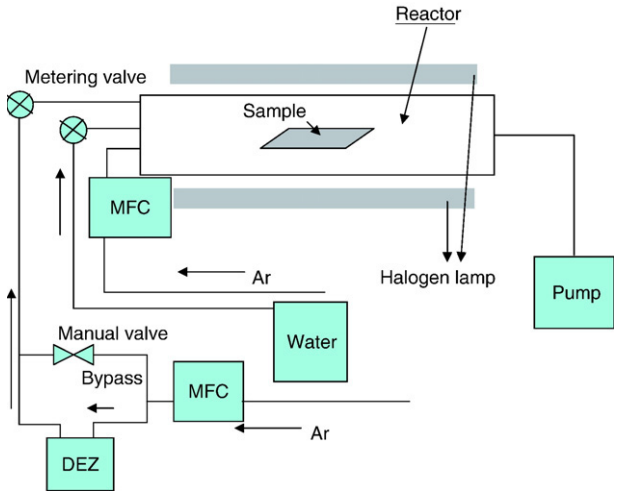

Fig. 1. Schematic drawing of hot wall type thermal ALD setup.

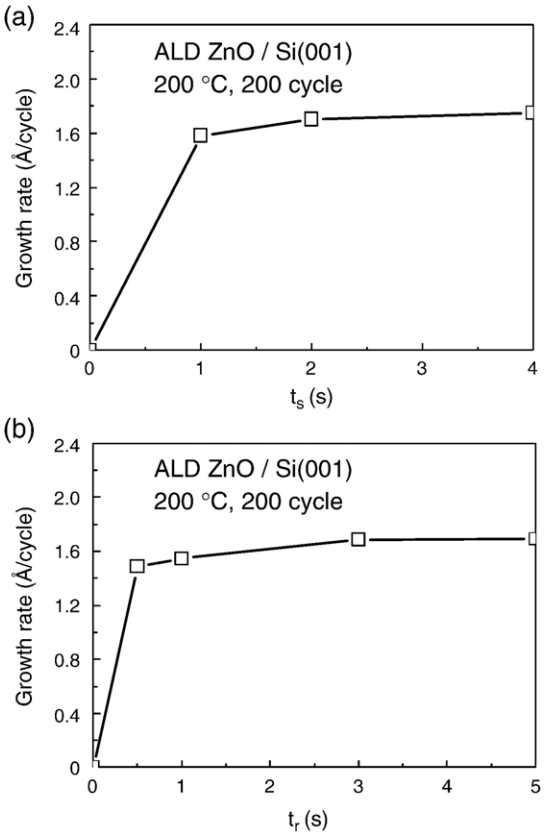

Fig. 2. Growth rates of thermal ALD ZnO prepared at T_s=200 °C on Si(001) as a function of (a) DEZ exposure time (t_s) and (b) water exposure time (t_r).

for 1 min. The thickness was routinely measured by ellipsometer (Rudolph auto ELII). The microstructures of the ZnO films were analyzed by X-ray diffraction (XRD) and cross-sectional transmission electron microscopy (JEOL, model JEM2010F). X-ray photoemission spectroscopy (XPS) was used for determining composition of ZnO films. For XPS, specimens were cleaned by Ar sputtering *in situ* for 4–5 nm in XPS chamber before measurement, and energy scan was carried out at around O 1s, Zn $2p_{3/2}$, and C 1s position with monochromatic AlK_{α} radiation source. The resistivity was routinely measured by a 4-point probe. Resistivity of ZnO was measured by 2-point probe method using Keithley 6517 electrometer when Samples have resistance Over 20 GΩ. For this measurement, we deposited Al through shadow mask to fabricate electrodes with various widths and lengths to eliminate the effects of contact resistance. Hall measurements were carried out for samples with resistivity lower than 20 GΩ. Hall measurement system was HL5500PC (Accent Optical Technologies) at Material Characterization Center in Korea Photonics Technology Institute.

3. Experimental results

3.1. ZnO deposition: ALD and sputtering

Fig. 2a shows the growth rates of ALD ZnO thin films, usually represented by thickness/cycle, as a function of DEZ exposure time (t_s) at T_s=200 °C on Si(001) substrates. No difference in

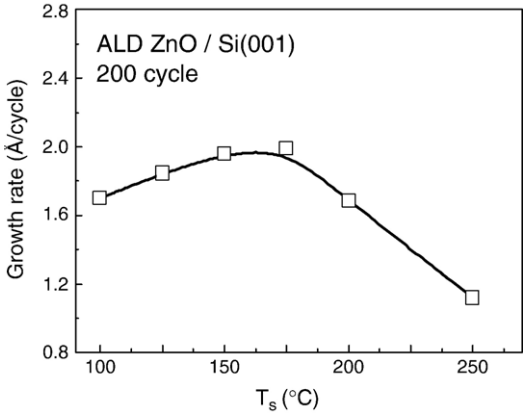

Fig. 3. Growth rates of thermal ALD ZnO on Si(001) as a function of growth temperature.

growth rate was observed for glass substrate. The growth rate increases with increasing t_s and saturates at ~1.7 Å/cycle at t_s>2 s. The saturation of growth rate indicates that a typical ALD mode growth is achieved by self-limited adsorption of DEZ at 200 °C. This growth rate is almost 0.3 Å/cycle higher than the previously reported value (1.4 Å/cycle) [22] and almost same as that of another report (1.65–1.7 Å/cycle) [25]. The growth rate change with water exposure time (t_r) also shows good saturation at t_r>3 s (Fig. 2b). From the thickness vs. the number of growth cycles data (not shown), almost no nucleation delay was observed on Si(001) and glass substrate.

In Fig. 3, the growth rates of ALD ZnO as a function of growth temperature are shown between T_s=100 and 250 °C. The growth rates increase with increasing temperatures at low growth temperature, reaching highest value of 2.0 Å/cycle at 175 °C. Above 175 °C, the growth rates decrease again to 1.12 Å/cycle at 250 °C. Similar trends were reported for ALD ZnO from DEZ and water [22,25]. This seems to be a typical behavior for ALD oxides from alkyl precursor and water. For example, ALD of Al_2O_3 from trimethyl aluminum and water, which has been intensively studied, shows almost same behavior [26,27]. At low growth temperature regions, the growth rate decreases with decreasing growth temperature probably due to the incomplete surface reaction [26]. However, when the surface reaction is not limited by the surface reaction of precursor, the surface hydroxyl density, acting as an adsorption site for precursors, determines the growth rate. Thus, at high growth temperature region, the surface hydroxyl density decreases with increasing growth temperature leading to reduction in the growth rate.

The XRD spectra of ALD ZnO thin films grown on glass substrates at growth temperatures between 100 and 250 °C are shown in Fig. 4. For all the samples, XRD spectra show that ALD ZnO films are composed of hexagonal wurtzite structure grains with strong (002) diffraction peak, implying that most of the *c*-axis of ZnO grains are arranged perpendicular to the

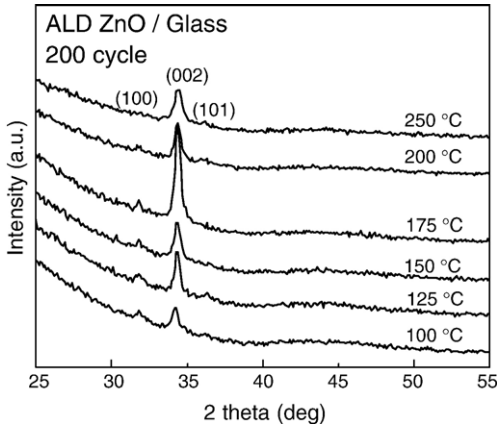

Fig. 4. XRD spectra of ALD ZnO thin films on glass prepared at different growth temperatures.

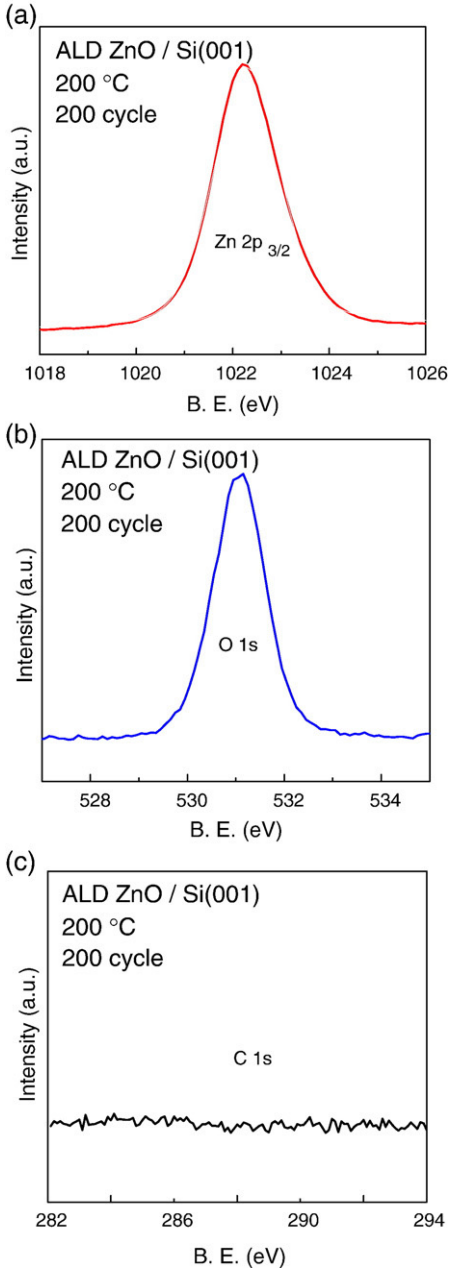

Fig. 5. XPS spectra of ALD ZnO thin films prepared at T_s=200 °C on Si(001) showing binding energy range of (a) Zn $2p_{3/2}$, (b) O 1s, and (c) C 1s.

substrate surface. However, (002) peak is especially dominant at high temperature over 175 °C. In several previous reports, (100) preferred orientation was usually observed for ALD ZnO at low growth temperatures [21–23]. However, (002) preferred orientation was reported to become stronger with increasing growth temperatures [22,25]. In fact, the preferred orientation of ALD ZnO has been reported to be largely dependent upon growth conditions. For example, (002) was the smallest for photo ALD [28] and addition of O_2 changes the preferred orientation from (100) to (002) [29].

Chemical bonding states and impurity contents in the films were investigated by XPS. Fig. 5 shows the XPS spectra of ALD ZnO film with thickness of 350 Å, prepared at 200 °C on silicon substrate. The sample was sputter-cleaned *in situ* right before the XPS measurement. The Zn 2p spectrum shown in Fig. 5a indicates that the peak position agrees well with the binding energy of Zn $2p_{3/2}$ from wurtzite ZnO phase, reported to be at 1022.4 eV [30] and the experimental data were well fitted with single Gaussian peak. No metallic Zn at 1021.5 eV was observed, indicating that all Zn atoms are in Zn_2^+ state [31]. The O 1s spectrum shown in Fig. 4b is composed of single component peak at 531.05 eV, which is associated with O_2^- ions in oxygen deficient state [31]. Same O 1s peak position was reported for metal organic CVD ZnO from DEZ and O_2 [32]. No additional peak related to O_2^- from excessive O_2 (533.3 eV) or O–H bonding (532.3 eV) was observed as a higher energy side tail [30,33]. Especially, no C contaminant was observed within detection limit of XPS (~1%), which would have been observed at 284.6 eV (Fig. 5c). So ALD ZnO produced in the current study is quite pure.

For comparison, ZnO thin films were deposited at room temperature by rf sputtering on Si (001) and glass substrates. The measured thicknesses of sputtered ZnO films are plotted in Fig. 6 as a function of rf sputtering power (from 50 to 150 W) for three different Ar pressure (0.2, 0.67, and 1.33 Pa) for 20 min of the total deposition time. Overall, the growth rates increase with increasing rf power since the number of atoms sputtered from the target increases with rf power. But the trend of growth rate change largely depends on the operating pressure. At low Ar pressure of 0.2 Pa, the growth rate increases up to 100 W, then remains almost

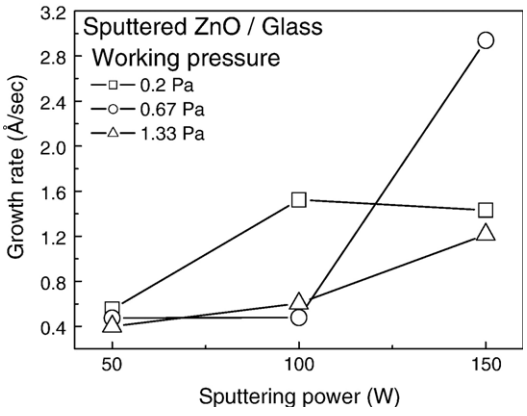

Fig. 6. Growth rate of rf sputtered ZnO as a function of sputtering power at working pressures of 0.2, 0.67, and 1.33 Pa. The depositions were done at room temperature.

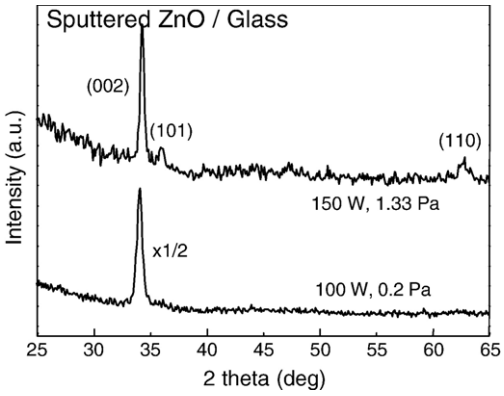

Fig. 7. XRD spectra of rf sputtered ZnO films prepared at 100 W, 0.2 Pa and 150 W, 1.33 Pa.

constant, while at a high pressure of 1.33 Pa, it increases almost monotonically with increasing rf power. The growth rate during rf sputtering is determined by the sputtering yield, target to substrate distance, and scattering of sputtered species. The exact reason for this complicated behavior of the growth rate dependence shown in Fig. 6 is not clearly understood yet.

ZnO films prepared by rf sputtering at all sputtering powers and working pressures show strong (002) preferred orientation (Fig. 7). Predominant (002) preferred orientation for room temperature rf sputtered ZnO is a general observation [15]. Compared to the ALD ZnO in Fig. 4, the sputtered ZnO seems

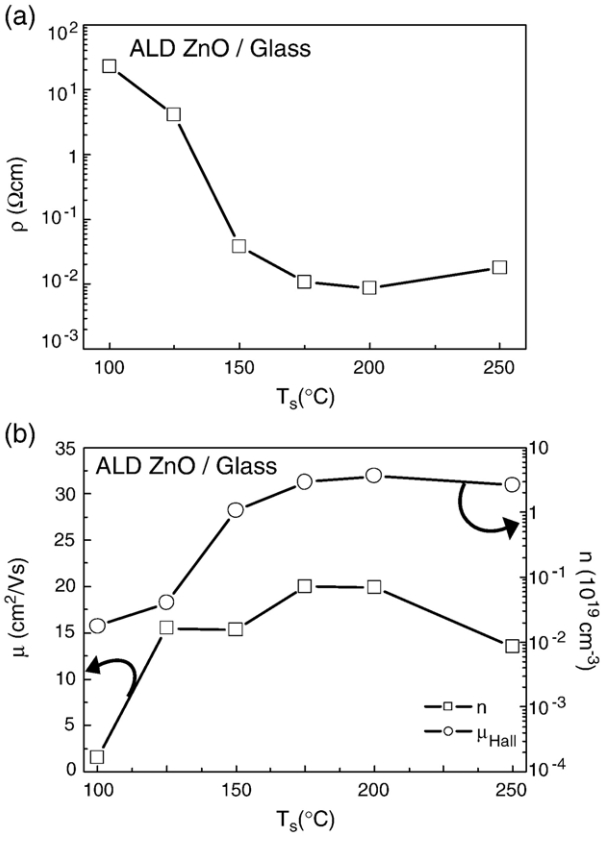

Fig. 8. (a) Resistivity and (b) mobility and carrier concentration of ALD ZnO on glass as a function of growth temperature.

to have more predominant (002) preferred orientation judging from the existence of small additional peaks for ALD ZnO. In contrast to a previous report showing amorphous phase formation at high sputtering power [15], we did not observe any amorphous film formation within all the investigated deposition parameter ranges. However, at 150 W sputtering power and under 1.33 Pa, small (101) and (110) diffraction peaks were also observed, indicating the microstructure is weakly dependent on growth parameters for rf sputtering of ZnO.

3.2. Comparisons of electrical properties

Room temperature electrical resistivity, carrier mobility, and carrier concentration were measured for both ALD and sputtered ZnO. The results of ALD ZnO thin films on glass substrates prepared at various growth temperatures are shown in Fig. 8. All the ALD ZnO thin films show n-type conductivity by Hall measurement system, agreeing with all previous studies on ZnO ALD [21,22,24,25]. Due to n-type carriers, the ALD ZnO films, even without any intentional doping, show relatively high conductivity. Fig. 8a shows that the resistivity at $T_s > 150$ °C is low at around 0.012–0.04 Ω cm. This relatively low resistivity can be attributed to the high mobility (13.5–20 cm^2/V s) and carrier concentration (1–3.7×10^{19} cm^{-3}) in the films. Similar values were reported in previous reports for undoped ALD ZnO films [22,25]. However, the resistivity increases with decreasing growth temperature, reaching 23.5 Ω cm at $T_s = 100$ °C. Especially at $T_s = 125$ °C, relatively high hall mobility (15 cm^2/V s) with low carrier concentration, 4.1×10^{17} cm^{-3}, was obtained. In a previous report [22], the increase in resistivity with the decrease in mobility and carrier concentration was observed with decreasing growth temperature below 140 °C, which is similar to our results [22]. However, in another report from ozone as a reactant, the opposite trend was observed at higher growth temperature region above 240 °C [25].

Fig. 9a is resistivity measurement results of rf sputtered ZnO thin films on glass at T_s = room temperature. In this case, since all the films were deposited at room temperature, the data are plotted as a function of rf sputtering power and operating pressure. At all Ar pressure studied, the resistivity values were measured to be high at 50 and 100 W. For these cases, the Hall measurements could not be done due to too large resistivity. Overall, the resistivity was above 1 kΩ cm, with highest values of almost 10 MΩ cm at 100 W, 0.2 Pa pressure. The carrier mobility and concentrations were measured for only the samples deposited at 150 W and plotted as a function of operating pressures. With small variations, the mobility was around 1.5–3.3 cm^2/V s with carrier concentrations of 4×10^{19} cm^{-3} to 2×10^{20} cm^{-3} range with n-type conductivity. Although we could not measure the carrier concentrations and mobilities for the films deposited at 50 and 100 W, the carrier concentrations should be very small estimated from almost 5 to 8 orders of magnitude higher resistivity than those at 150 W, since the mobility difference should not be very large.

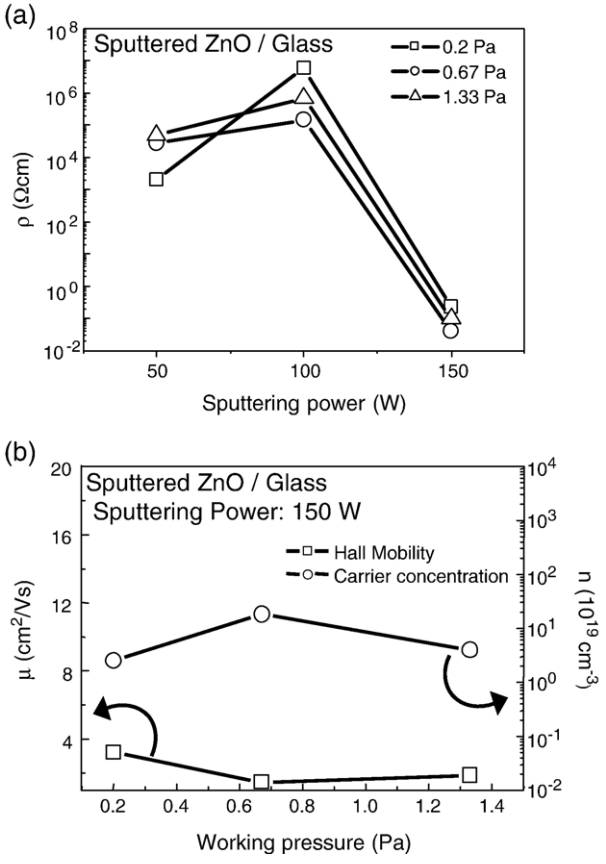

Fig. 9. (a) Resistivity as a function of sputtering power and (b) hall mobility and carrier concentration as a function of working pressure for rf sputtered ZnO on glass prepared at room temperature.

4. Discussions

Until now, the exact physical origin for n-type conductivity in ZnO is not known. Most plausibly, the origin of n-type conduction is the inherent defects in the film such as oxygen vacancies or interstitial Zn atoms. However, other possibility due to H impurity in the films cannot be excluded [34]. Usually, the low carrier concentration is expected to result in high mobility, which is contrary to the current observations for ALD ZnO. The single crystal ZnO can exhibit very high mobility up to 300 cm^2/V s [35]. Thus, the low mobility of polycrystalline ZnO thin films has been often attributed to the Schottky barrier at the grain boundary. In other words, the charges trapped at the grain boundaries make high-energy barrier for carrier transport, producing low mobility. So although the carrier concentration is low and the mobility inside the grain may be high for ALD ZnO films prepared at low growth temperatures, the existence of high-energy barrier at grain boundary seems to result in this low mobility. In contrast, the relatively small number of charges trapped at grain boundary results in higher mobility for ZnO films at higher growth temperature, although the carrier concentration is high. The exact reason for this difference in grain boundary energy barrier depending on growth temperature is not understood yet. One possibility is that more impurities are gathered at grain boundaries at lower growth temperature, leading to lower mobility.

Meanwhile, the sputtered ZnO thin films prepared at 50–100 W rf sputtering power should have very small inherent defect concentration, judging from very high resistivity at these growth conditions. However, the films deposited at high power have low resistivity with high carrier concentrations. One possible explanation for this observation is that inherent defects are prone to be generated at high sputtering power due to the arrival of energetic depositing particles, leading to higher carrier concentration. However, considering that the sputtered power used in the present study is not that high, more plausible reason may be that the inherent defects creation is thermodynamically preferable. Thus, kinetically controlled deposition environment at lower sputtering power produces films with lower carrier concentrations.

For application as an active channel layer of TTFT, ZnO thin film should have high mobility. In this regard, the ALD ZnO prepared at 175 °C, which has highest mobility, has great benefits. But the Hall measurements indicate that these films have too high carrier concentration. This high carrier concentration will contribute to large off current. Considering that the on–off current ratio of active layer should be at least 10^6, these films may not be good for TFT applications. In this regard, the ALD ZnO films deposited at low concentration with relatively low off current may be better for TFT applications, while they could suffer from low mobility. All these results indicate that the ALD process should be properly modified for fabricating ZnO active layers for TFT fabrication. These include changes in reactants and precursors, the use of radical-based ALD, or proper doping of extra elements. For example, much lower carrier concentrations were observed for O_3-based ZnO ALD [25]. Sputtered ZnO, especially at low rf sputtering powers, seems more promising for TFT applications at this stage. Using similar growth techniques, TTFT with reasonably good characteristics was fabricated using these kinds of high-resistivity ZnO films in the previous reports [15]. However, with the absence of device characteristics using the ZnO films prepared in this study, decisive predictions cannot be done at this time. Modifications of ALD and sputtering processes are currently under investigation. Initial results seem promising, indicating that electrical properties can be tuned by changing key growth parameters.

5. Conclusions

ZnO thin films were prepared by thermal ALD and rf sputtering technique at low growth temperatures. XPS results of ALD ZnO show no carbon contamination in the films without O–H bond. Both ALD and sputtered ZnO thin films have generally (002) preferred orientations, while more predominant *c*-axis preferred orientation was observed in sputtering. The electrical properties of ZnO films were found to be largely dependent on growth parameters. For ALD ZnO, resistivity changes up to two orders of magnitude were observed depending on growth temperatures. The sputtered ZnO films have shown resistivities spanning over 9 orders of magnitude depending on sputtering power. Due to relatively high carrier concentrations in ALD ZnO, proper modifications in deposition process should be carried out to be used as an active channel layer in TFT.

Acknowledgements

This work was supported by Samsung SDI, POSTECH Core Research Program, Korean Research Foundation Grant funded by the Korean Government(MOEHRD)(KRF-2005-005-J13102), and POSRIP. The authors are deeply thankful to Prof. Wang Chul Zin for help in ellipsometry analysis.

References

[1] S.P.S. Arya, O.N. Srivastava, Cryst. Res. Technol. 23 (1988) 669.
[2] J.K. Srivastava, L. Agrawal, B. Bhattacharyya, J. Electrochem. Soc. 11 (1989) 3414.
[3] Z.C. Jin, C.G. Granqvist, Proc. SPIE 21 (1987) 827.
[4] C. Lee, K. Lim, J. Song, Sol. Energy Mater. Sol. Cells 43 (1996) 37.
[5] S.J. Pearton, D.P. Norton, K. Ip, Y.W. Heo, T. Steiner, Prog. Mater. Sci. 50 (2005) 293.
[6] H.S. Bae, S. Im, Thin Solid Films 469 (2004) 75.
[7] S.K. Hazra, S. Basu, Solid State Electron. 49 (2005) 1158.
[8] S. Muthukumar, C.R. Gorla, N.W. Emanetoglu, S. Liang, Y. Lu, J. Cryst. Growth 225 (2001) 197.
[9] V. Assuncao, E. Fortunato, A. Marques, H. Aguas, I. Ferreira, M.E.V. Costa, R. Martins, Thin Solid Films 427 (2003) 401.
[10] S. Jager, B. Szyszka, J. Szczyrbowski, G. Bauer, Surf. Coat. Technol. 98 (1998) 1304.
[11] E. Fortunato, P. Barquinha, A. Pimentel, A. Gonçalves, A. Marques, L. Pereira, R. Martins, Thin Solid Films 487 (2005) 205.
[12] H. Cheng, C. Chen, C. Lee, Thin Solid Films 498 (2006) 142.
[13] R.L. Hoffman, J. Appl. Phys. 95 (2004) 5813.
[14] P. Barquinha, E. Fortunato, A. Gonçalves, A. Pimentel, A. Marques, L. Pereira, R. Martins, Superlattices Microstruct. 39 (2006) 319.
[15] E. Fortunato, P. Barguinha, A. Pimentel, A. Gonçalves, A. Marques, L. Pereira, R. Martins, Adv. Mater. 17 (2005) 590.
[16] P.F. Carcia, R.S. McLean, M.H. Reilly, G. Nunes Jr., Appl. Phys. Lett. 82 (2003) 1117.
[17] S. Masuda, K. Kitamura, Y. Okumura, S. Miyatake, J. Appl. Phys. 93 (2003) 1624.
[18] Y. Ohyam, T. Niwa, T. Ban, Y. Takahashi, Jpn. J. Appl. Phys. 297 (2001) 40.
[19] A.N. Banerjee, C.K. Ghosh, K.K. Chattopadhyay, H. Minoura, A. Sarkar, A. Akiba, A. Kamiya, T. Endo, Thin Solid Films 496 (2006) 112.
[20] H. Kim, J. Vac. Sci. Technol., B 21 (2003) 2231.
[21] A. Yamada, B. Sang, M. Konagai, Appl. Surf. Sci. 112 (1997) 216.
[22] V. Lujala, J. Skarp, M. Tammenmaa, T. Suntola, Appl. Surf. Sci. 82–83 (1994) 34.
[23] E. Yousfi, J. Fouache, D. Lincot, Appl. Surf. Sci. 153 (2000) 223.
[24] A.W. Ott, R.P.H. Chang, Mater. Chem. Phys. 58 (1999) 132.
[25] S.K. Kim, C.S. Hwang, S. Ko Park, S.J. Yun, Thin Solid Films 478 (2005) 103.
[26] R. Matero, A. Rhatu, M. Ritala, M. Leskela, T. Sajavaara, Thin Solid Films 368 (2000) 1.
[27] R.L. Pruunen, J. Appl. Phys. 97 (2005) 121301.
[28] Y. Yamamoto, K. Saito, K. Takahashi, M. Konagai, Sol. Energy Mater. Sol. Cells 65 (2001) 125.
[29] S.-H. Ko Park, Y.E. Lee, J. Mater. Sci. 39 (2004) 2195.
[30] M. Islam, T.B. Glosh, K.L. Chopra, H.N. Acharya, Thin Solid Films 280 (1996) 20.
[31] M. Chen, X. Wang, Y.H. Yu, Z.L. Pei, X.D. Bai, C. Sun, R.F. Huang, L.S. Wen, Appl. Surf. Sci. 158 (2000) 134.
[32] Y. Zhang, G. Du, X. Wang, W. Li, X. Yang, Y. Ma, B. Zhao, H. Yang, D. Liu, S. Yang, J. Cryst. Growth 252 (2003) 180.
[33] B.J. Coppa, R.F. Davis, Appl. Phys. Lett. 82 (2003) 400.
[34] Z. Zhou, K. Kato, T. Komaki, M. Yoshino, H. Yakawa, M. Morinaga, Int. J. Hydrogen Energy 29 (2004) 323.
[35] Ü. Özgür, I. Alivov, C. Liu, A. Teke, M.A. Reshchikov, S. Dogan, V. Avrutin, S.-J. Cho, H. Mokoç, J. Appl. Phys. 98 (2005) 041301.